Inorg. Chem. **2008**, *47*, 5951−5962

Solid-State Molecular Rotators of Anilinium and Adamantylammonium in $[Ni(dmit)_2]^-$ Salts with Diverse Magnetic Properties

Tomoyuki Akutagawa,*,†,‡,§ Daisuke Sato,‡ Hiroyuki Koshinaka,‡ Masaaki Aonuma,‡ Shin-ichiro Noro,†,‡ Sadamu Takeda,|| and Takayoshi Nakamura*,†,‡,§

Research Institute for Electronic Science, Hokkaido University, Sapporo 060-0812, Japan, Graduate School of Environmental Earth Science, Hokkaido University, Sapporo 060-0810, Japan, CREST, Japan Science and Technology Agency (JST), Kawaguchi 332-0012, Japan, and Graduate School of Science, Hokkaido University, Sapporo 060-0810, Japan

Received February 13, 2008

Supramolecular rotators of hydrogen-bonding assemblies between anilinium ($Ph\text{-}NH_3^+$) or adamantylammonium ($AD\text{-}NH_3^+$) and dibenzo[18]crown-6 (DB[18]crown-6) or *meso*-dicyclohexano[18]crown-6 (DCH[18]crown-6) were introduced into $[Ni(dmit)_2]$ salts ($dmit^{2-}$ is 2-thioxo-1,3-dithiole-4,5-dithiolate). The ammonium moieties of $Ph-NH_3^+$ and $AD-NH_3^+$ cations were interacted through $N-H^+\sim O$ hydrogen bonding with the six oxygen atoms of crown ethers, forming 1:1 supramolecular rotator−stator structures. X-ray crystal-structure analyses revealed a jackknife-shaped conformation of DB[18]crown-6, in which two benzene rings were twisted along the same direction, in $(Ph-NH_3^+)(DB[18]crown\text{-}6)[Ni(dmit)_2]^-$ (**1**) and $(AD-NH_3^+)(DB[18]crown\text{-}6)[Ni(dmit)_2]^-$ (**3**), whereas the conformational flexibility of two dicyclohexyl rings was observed in $(Ph-NH_3^+)(DCH[18]crown\text{-}6)[Ni(dmit)_2]^-$ (**2**) and $(AD-NH_3^+)(DCH[18]crown\text{-}6)[Ni(dmit)_2]^-$ (**4**). Sufficient space for the molecular rotation of the adamantyl group was achieved in the crystals of salts **3** and **4**, whereas the rotation of the phenyl group in salts **1** and **2** was rather restricted by the nearest neighboring molecules. The rotation of the adamantyl group in salts **3** and **4** was evidenced from the temperature-dependent wide-line ^1H NMR spectra, dielectric properties, and X-ray crystal structure analysis. ab initio calculations showed that the potential energy barriers for the rotations of adamantyl groups in salts **3** ($\Delta E \approx 18$ kJmol^{-1}) and **4** ($\Delta E \approx 15$ kJmol^{-1}) were similar to those of ethane ($\sim$12 kJmol^{-1}) and butane (17−25 kJmol^{-1}) around the C−C single bond, which were 1 order of magnitude smaller than those of phenyl groups in salts **1** ($\Delta E \approx 180$ kJmol^{-1}) and **2** ($\Delta E \approx 340$ kJmol^{-1}). 1D or 2D $[Ni(dmit)_2]^-$ anion arrangements were observed in the crystals according to the shape of crown ether derivatives. The 2D weak intermolecular interactions between $[Ni(dmit)_2]^-$ anions in salts **1** and **3** led to Curie−Weiss behavior with weak antiferromagnetic interaction, whereas 1D interactions through lateral sulfur−sulfur atomic contacts between $[Ni(dmit)_2]^-$ anions were observed in salts **2** and **4**, whose magnetic behaviors were dictated by ferromagnetic (salt **2**) and singlet−triplet (salt **4**) intermolecular magnetic interactions, respectively.

Introduction

Flexible molecules such as rotaxanes and catenanes, which possess several thermodynamically stable and/or metastable conformations, are among the useful building blocks for constructing molecular machines, such as motors and shuttles.[1] Coupling the molecular conformational change, especially molecular rotational motion, with electronic func-

* To whom correspondence should be addressed. Phone: +81-11-706-2884, Fax: +81-11-706-4972, E-mail: takuta@es.hokudai.ac.jp (A.T.), tnaka@es.hokudai.ac.jp (T.N.).
† Research Institute for Electronic Science, Hokkaido University.
‡ Graduate School of Environmental Earth Science, Hokkaido University.
§ CREST, Japan Science and Technology Agency (JST).
|| Graduate School of Science, Hokkaido University.

(1) (a) Lindoy, L. F.; Atkinson, I. M. *Self-Assembly in Supramolecular Systems*; Stoddart, J. F., Ed.; RSC: Cambridge, 2000. (b) *Molecular Switches*; Feringa, B. L., Ed.; Wiley-VCH: Weinheim, Germany, 2001. (c) *Molecular Machines and Motors*; Sauvage, J.-P.,. Ed.; Springer: Berlin, 2001. (d) *Molecular Devices and Machines*; Balzani, V., Venturi, M., Credi, A., Eds.; Wiley-VCH: Weinheim, Germany, 2003. (e) Molecular Machines Special Issue. *Acc. Chem. Res.* **2001**, *34*, 412.

10.1021/ic800271m CCC: $40.75
Published on Web 05/28/2008

tions will enable us to construct molecular machines, whose intramolecular rotary motion is controllable through outer stimuli, such as electromagnetic field, photoirradiation, and redox reactions.[1,2] A large number of molecular rotary machines have already been developed that allow unidirectional rotation in the solution phase using rotaxane and catenane structures.[1–4] Molecular machines have a potential to realize collective transport systems of electrons, protons, ions, and so forth. For example, ATPase in cell membranes is a well-known biological molecular motor,[5] in which the ionic channel, proton relay, and unidirectional molecular rotation are coupled to each other, forming a proton pump with high-energy conversion efficiency.[5] One important feature of biological motors is that they are aligned in the same direction in the cell membrane so that they achieve directional proton transport through unidirectional rotation by consuming ATP. Although such a complex molecular system is difficult to construct artificially, solid-state molecular motors are promising model systems for mimicking biological functions from the viewpoint of directional alignment of rotators. To the best of our knowledge, unidirectional molecular rotation has not yet been achieved in the solid state. In the solid state, structural isomerizations such as thermal, photo-, and chemical reactions for achieving unidirectional molecular rotations are very difficult, owing to the steric hindrance between the nearest-neighboring molecules. An entirely different approach from that for the solution phase is necessary to construct solid-state molecular motors.

Although the solid-state molecular rotators that have been reported to date are far from actual molecular motors, several important functions have been achieved, which could pave the way to solid-state molecular motors.[6,8] The potential energy for molecular rotation is generally dominated by steric hindrance between nearest-neighboring molecules in the solid state, and thus the rotational motion of large rotators, such as the phenyl ring, is affected by the crystalline environment unlike that of small rotators, such as the methyl group.[9,10] A promising approach to reducing the rotation energy barrier in the solid state has been reported for molecular turnstiles, merry-go-rounds, gyroscopes, and so forth,[6,11,12] where the rotator was covalently bound to the bulky stators to preserve enough space for the 360 degree rotation in the crystal. These design principles have been employed to construct a variety of crystalline rotators.[6] Plastic crystals represent another

(2) (a) Balzani, V.; Credi, A.; Raymo, F. M.; Stoddart, J. F. *Angew. Chem., Int. Ed.* **2000**, *39*, 3348. (b) Kottas, G. S.; Clarke, L. I.; Horinek, D.; Michl, J. *Chem. Rev.* **2005**, *105*, 1281. (c) Kay, E. R.; Leigh, D. A.; Zerbetto, F. *Angew. Chem., Int. Ed.* **2007**, *46*, 72.

(3) (a) Bissell, R. A.; Córdova, E.; Kaifer, A. E.; Stoddart, J. F. *Nature* **1994**, *369*, 133. (b) Martínez-Díaz, M.-V.; Spencer, N.; Stoddart, J. F. *Angew. Chem., Int. Ed.* **1997**, *36*, 1904. (c) Bermudez, V.; Capron, N.; Gase, T.; Gatti, F. G.; Kajzar, F.; Leigh, D. A.; Zerbetto, F.; Zhang, S. *Nature* **2000**, *406*, 608. (d) Brouwer, A. M.; Frochot, C.; Gatti, F. G.; Leigh, D. A.; Mottier, L.; Paolucci, F.; Roffia, S.; Wurpel, G. W. H. *Science* **2001**, *291*, 2124. (e) Collin, J. P.; Dietrich-Buchecker, C.; Gaviña, P.; Jimenez-Molero, M. C.; Sauvage, J.-P. *Acc. Chem. Res.* **2001**, *34*, 477. (f) Jimenez-Molero, M. C.; Dietrich-Buchecker, C.; Sauvage, J.-P. *Chem. Commun.* **2003**, 1613. (g) Schneider, H. J.; Tianjun, L.; Lomazdze, N. *Angew. Chem., Int. Ed.* **2003**, *42*, 3544. (h) Zheng, X.; Mulcahy, M. E.; Horinek, D.; Galeotti, F.; Magnera, T. F.; Michl, J. *J. Am. Chem. Soc.* **2004**, *126*, 4540. (i) Hernández, J. V.; Kay, E. R.; Leigh, D. A. *Science* **2004**, *306*, 1532. (j) Fletcher, S. P.; Dumur, F.; Pollard, M. M.; Feringa, B. L. *Science* **2005**, *310*, 80. (k) Hawthorne, M. F.; Zink, J. I.; Skelton, J. M.; Bayer, M. J.; Liu, C.; Livshits, E.; Baer, R.; Neuhauser, D. *Science* **2004**, *303*, 1849.

(4) (a) Kelly, T. R.; Silva, H. D.; Silva, R. A. *Nature* **1999**, *401*, 150. (b) Koumura, N.; Zijlstra, R. W. J.; van Delden, R. A.; Harada, N.; Feringa, B. L. *Nature* **1999**, *401*, 152. (c) Kelly, T. R.; Silva, R. A.; Silva, H. D.; Jasmin, S.; Zhao, Y. *J. Am. Chem. Soc.* **2000**, *122*, 6935. (d) Feringa, B. L. *Acc. Chem. Res.* **2001**, *34*, 504. (e) Koumura, N.; Geertsema, E. M.; van Gelder, M. B.; Meetsma, A.; Feringa, B. L. *J. Am. Chem. Soc.* **2002**, *124*, 5037. (f) van Delden, R. A.; Koumura, N.; Harada, N.; Feringa, B. L. *Proc. Natl. Acad. Sci. U.S.A.* **2002**, *99*, 4945. (g) Feringa, B. L.; van Delden, R. A.; ter Wiel, M. K. J. *Pure Appl. Chem.* **2003**, *75*, 563. (h) Leigh, D. A.; Wong, J. K. Y.; Dehez, F.; Zerbetto, F. *Nature* **2003**, *424*, 174. (i) van Delden, R. A.; Hurenkamp, J. H.; Feringa, B. L. *Chem.—Eur. J.* **2003**, *9*, 2845.

(5) Stryer, L. *Biochemistry*; Freeman: New York, 1995.

(6) (a) Dominguez, Z.; Dang, H.; Strouse, M. J.; Garcia-Garibay, M. A. *J. Am. Chem. Soc.* **2002**, *124*, 2398. (b) Godinez, C. E.; Zepeda, G.; Garcia-Garibay, M. A. *J. Am. Chem. Soc.* **2002**, *124*, 4701. (c) Dominguez, Z.; Dang, H.; Strouse, M. J.; Garcia-Garibay, M. A. *J. Am. Chem. Soc.* **2002**, *124*, 7719. (d) Dominguez, Z.; Khuong, T. V.; Dang, H.; Sanrame, C. N.; Nuñez, J. E.; Garcia-Garibay, M. A. *J. Am. Chem. Soc.* **2003**, *125*, 8827. (e) Dominguez, Z.; Khuong, T. V.; Dang, H.; Sanrame, C. N.; Nuñez, J. E.; Garcia-Garibay, M. A. *J. Am. Chem. Soc.* **2003**, *125*, 8827. (f) Godinez, C. E.; Zepeda, G.; Mortko, C. J.; Dang, H.; Garcia-Garibay, M. A. *J. Org. Chem.* **2004**, *69*, 1652. (g) Khuong, T. V.; Zepeda, G.; Ruiz, R.; Khan, S. I.; Garcia-Garibay, M. A. *Cryst. Growth Des.* **2004**, *4*, 15. (h) Karlen, S. D.; Ortiz, R.; Chapman, O. L.; Garcia-Garibay, M. A. *J. Am. Chem. Soc.* **2005**, *127*, 6554. (i) Karlen, S. D.; Garcia-Garibay, M. A. *Chem. Commun.* **2005**, 189. (j) Horansky, R. D.; Clarke, L. I.; Price, J. C.; Khuong, T. V.; Jarowski, P. D.; Garcia-Garibay, M. A. *Phys. Rev. B* **2005**, *72*, 014302. (k) Karlen, S. D.; Ortiz, R.; Chapman, O. L.; Garcia-Garibay, M. A. *J. Am. Chem. Soc.* **2005**, *127*, 6554. (l) Karlen, S. D.; Khan, S. I.; Garcia-Garibay, M. A. *Cryst. Growth Des.* **2005**, *5*, 53. (m) Horansky, R. D.; Clarke, L. I.; Winston, E. B.; Price, J. C.; Karlen, S. D.; Jarowski, P. D.; Santillan, R.; Garcia-Garibay, M. A. *Phys. Rev. B.* **2006**, *74*, 054306. (n) Karlen, S. D.; Godinez, C. E.; Garcia-Garibay, M. A. *Org. Lett.* **2006**, *8*, 3417. (o) Garcia-Garibay, M. A. *Proc. Natl. Acad. Sci. U.S.A.* **2005**, *102*, 10771. (p) Khuong, T. V.; Nuñez, J. E.; Godinez, C. E.; Garcia-Garibay, M. A. *Acc. Chem. Res.* **2006**, *39*, 413. (q) Jarowski, P. D.; Houk, K. N.; Garcia-Garibay, M. A. *J. Am. Chem. Soc.* **2007**, *129*, 3110. (r) Khuong, T. V.; Dang, H.; Jarowski, P. D.; Maverick, E. F.; Garcia-Garibay, M. A. *J. Am. Chem. Soc.* **2007**, *129*, 839. (s) Shima, T.; Hampel, F.; Gladysz, J. A. *Angew. Chem., Int. Ed.* **2004**, *43*, 5337. (t) Wang, L.; Shima, T.; Hampel, F.; Gladysz, J. A. *Chem. Commun.* **2006**, 4075. (u) Skopek, K.; Hershberger, M. C.; Gladysz, J. A. *Coord. Chem. Rev.* **2007**, *251*, 1723. (v) Hess, G. D.; Hampel, F.; Gladysz, J. A. *Organometallics* **2007**, *26*, 5129. (w) Setaka, W.; Ohmizu, S.; Kabuto, C.; Kira, M. *Chem. Lett.* **2007**, 1076.

(7) (a) Clarke, L. I.; Horinek, D.; Kottas, G. S.; Varaksa, N.; Magnera, T. F.; Hinderer, T. P.; Horansky, R. D.; Michl, J.; Price, J. C. *Nanotechnology* **2002**, *13*, 533. (b) How, S.; Sagara, T.; Xu, D.; Kelly, T. R.; Ganz, E. *Nanotechnology* **2003**, *14*, 566. (c) Gardinier, J. R.; Pellechia, P. J.; Smith, M. D. *J. Am. Chem. Soc.* **2005**, *127*, 12449. (d) Horike, S.; Matsuda, R.; Tanaka, D.; Matsubara, S.; Mizuno, M.; Endo, K.; Kitagawa, S. *Angew. Chem., Int. Ed.* **2006**, *45*, 7226. (e) Horinek, D.; Michl, J. *Proc. Natl. Acad. Sci. U.S.A.* **2005**, *102*, 14175.

(8) (a) Akutagawa, T.; Shitagami, K.; Nishihara, S.; Takeda, S.; Hasegawa, T.; Nakamura, T.; Hosokoshi, Y.; Inoue, K.; Ikeuchi, S.; Miyazaki, Y.; Saito, K. *J. Am. Chem. Soc.* **2005**, *127*, 4397. (b) Ikeuchi, S.; Miyazaki, Y.; Takeda, S.; Akutagawa, T.; Nishihara, S.; Nakamura, T.; Saito, K. *J. Chem. Phys.* **2005**, *123*, 044514. (c) Sato, D.; Akutagawa, T.; Takeda, S.; Noro, S.; Nakamura, T. *Inorg. Chem.* **2007**, *46*, 363. (d) Nishihara, S.; Akutagawa, T.; Sato, D.; Takeda, S.; Noro, S.; Nakamura, T. *Chem. Asian J.* **2007**, *2*, 1983.

(9) (a) *The Plastically Crystalline State*; Sherwood, J. N. Ed.; John Wiley & Sons: Chichester, 1979. (b) Hamilton, W. C.; Ibers, J. A. *Hydrogen Bonding in Solid*; W. A. Benjamin Inc.: New York, 1968.

(10) (a) Rice, D. M.; Meinwald, Y. C.; Scheraga, H. A.; Griffin, R. G. *J. Am. Chem. Soc.* **1987**, *109*, 1636. (b) Wendeler, M.; Fattah, J.; Twyman, J. M.; Edwards, J. A.; Dobson, M. C.; Heyes, J. S.; Prout, K. *J. Am. Chem. Soc.* **1997**, *119*, 9793. (c) Casarini, D.; Lunazzi, L.; Mazzanti, A. *Angew. Chem., Int. Ed.* **2001**, *40*, 2536.

(11) (a) Buchanan, G. W.; Kirby, R. A.; Ripmeester, J. A.; Ratcliffe, C. I. *Tetrahedron Lett.* **1987**, *28*, 4783. (b) Ratcliffe, C. I.; Ripmeester, J. A.; Buchanan, G. W.; Denike, J. K. *J. Am. Chem. Soc.* **1992**, *114*, 3294.

(12) Bedard, T. C.; Moore, J. S. *J. Am. Chem. Soc.* **1995**, *117*, 10662.

Scheme 1. Molecular Structures of Anilinium ($Ph-NH_3^+$), Adamantylammonium ($AD-NH_3^+$), Dibenzo[18]crown-6 (DB[18]crown-6), *meso*-Dicyclohexano[18]crown-6 (DCH[18]crown-6), and $[Ni(dmit)_2]$[a]

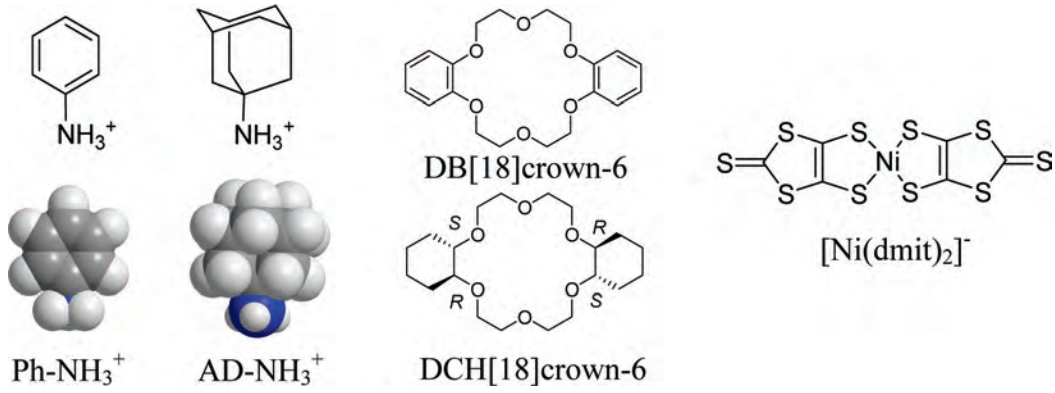

[a] Molecular structures of bottom $Ph-NH_3^+$ and $AD-NH_3^+$ were shown in the CPK representation.

possibility.[9] In plastic crystals, relatively large molecules, such as cyclohexane, adamantane (AD), and C_{60}, can rotate, keeping the center of gravity in the crystal lattice.[9] A peculiar feature of these plastic crystals is their high conformational flexibility and/or isotropic molecule shape. Such molecules are suitable candidates for constructing crystalline rotators.

We have employed the supramolecular cation approach based on crown ethers to construct rotators in the crystals of magnetic $[Ni(dmit)_2]$ salts ($dmit^{2-}$ is 2-thioxo-1,3-dithiole-4,5-dithiolate).[8,13] The crown ether supramolecular cation$-[Ni(dmit)_2]$ approach has several advantages: (i) the combination of organic and/or inorganic cations and crown ethers yields diverse molecular rotator structures, (ii) one-pot synthesis of rotator−stator structures by self-assembly processes through selective cation recognition by crown ethers becomes possible, and (iii) magnetically and electrically active $[Ni(dmit)_2]$ anions can coexist with the rotators. Such hybrid solids between the molecular rotators and magnetic spin (or conduction electrons of $[Ni(dmit)_2]$) has a potential to show peculiar electronic functions coupled with the molecular motion.[14]

We first reported the molecular rotator of [18]crown-6 in the salt $Cs^+_2([18]crown\text{-}6)_3[Ni(dmit)_2]^-_2$.[8a] In this salt, the rotation of [18]crown-6 was coupled with the magnetic properties of the $[Ni(dmit)_2]^-$ assembly. More recently, we reported the supramolecular rotators in $(Ph-NH_3^+)([18]crown\text{-}6)[Ni(dmit)_2]^-$ and $(AD-NH_3^+)([18]crown\text{-}6)[Ni(dmit)_2]^-$ ($Ph-NH_3^+$ and $AD-NH_3^+$ were anilinium and adamantylammonium, respectively).[8c,d] In these salts, dual-mode rotations, that is, organic ammoniums and [18]crown-6 with different rotation frequencies, were confirmed by solid-state ^1H and ^2H NMR measurements. Reflecting the isotropic molecular structure of the adamantyl group, the rotation speed of the adamantyl group was much faster than that of the phenyl group in the solid state.[8c,d] However, in previous salts, the [18]crown-6 itself acted as the rotator and/or stator simultaneously. Here, we report new supramolecular solid-state rotators of phenyl and adamantyl groups fixed on bulky stators of dibenzo[18]crown-6 (DB[18]crown-6) and *meso*-dicyclohexano[18]crown-6 (DCH[18]crown-6). Four new single crystals of $(Ph-NH_3^+)$(DB[18]crown-6)$[Ni(dmit)_2]^-$ (**1**), $(Ph-NH_3^+)$(DCH[18]crown-6)$[Ni(dmit)_2]^-$ (**2**), and $(AD-NH_3^+)$(DB[18]crown-6)$[Ni(dmit)_2]^-$ (**3**), and $(AD-NH_3^+)$(DCH[18]crown-6)$[Ni(dmit)_2]^-$ (**4**) were prepared (Scheme 1). The rotation of bulky crown ethers was completely suppressed in the solid state, whereas an extremely low potential energy barrier (15−18 $kJmol^{-1}$) for the rotation of the adamantyl group was confirmed in the solid state. Diverse magnetism from antiferromagnetic to ferromagnetic coupling depended on the $[Ni(dmit)_2]^-$ ($S = {}^1/_2$) arrangements through the lateral S̃–S contacts within the crystals.

Experimental Section

$(Ph-NH_3^+)(BF_4^-)$. An aqueous 42% solution of HBF_4 (9.8 mmol) was slowly dropped into aniline (10 mmol) in CH_3CN (30 mL) over a period of 20 min. The reaction solvent was removed by reducing of pressure, and then white powder was recrystallized from $CHCl_3-CH_3CN$. Elemental analysis. Calcd C: 39.82, H: 4.46, N: 7.74. Found. C: 39.71, H: 4.45, N: 7.74.

$(AD-NH_3^+)(BF_4^-)$. An aqueous 42% solution of HBF_4 was slowly dropped into adamantylamine (0.76 g, 5 mmol) in CH_3OH (20 mL) over a period of 20 min. During this reaction, the reaction solution was adjusted to pH ∼7 and stirred for 30 min at room

(13) (a) Takamatsu, N.; Akutagawa, T.; Hasegawa, T.; Nakamura, T.; Inabe, T.; Fujita, W.; Awaga, K. *Inorg. Chem.* **2000**, *39*, 870. (b) Akutagawa, T.; Nishihara, S.; Takamatsu, N.; Hasegawa, T.; Nakamura, T.; Inabe, T. *J. Phys. Chem. B* **2000**, *104*, 5871. (c) Akutagawa, T.; Takamatsu, N.; Shitagami, K.; Hasegawa, T.; Nakamura, T.; Inabe, T. *J. Mater. Chem.* **2001**, *11*, 2118. (d) Akutagawa, T.; Hashimoto, A.; Nishihara, S.; Hasegawa, T.; Nakamura, T. *J. Supra. Chem.* **2002**, *2*, 175. (e) Akutagawa, T.; Hashimoto, A.; Nishihara, S.; Hasegawa, T.; Nakamura, T. *J. Phys. Chem. B.* **2003**, *107*, 66. (f) Nishihara, T.; Akutagawa, T.; Hasegawa, T.; Nakamura, T. *Inorg. Chem.* **2003**, *42*, 2480. (g) Akutagawa, T.; Matsuura, K.; Nishihara, S.; Noro, S.; Nakamura, T. *Eur. J. Inorg. Chem.* **2005**, 3271. (h) Akutagawa, T.; Matsuura, K.; Hashimoto, A.; Nakamura, T. *Inorg. Chem.* **2005**, *44*, 4454.

(14) (a) Ramos, J. J. M.; Sousa, R. J. C.; Correia, N. T.; Dionsio, M. S. C. *Ber. Bunsenges. Phys. Chem.* **1996**, *100*, 571. (b) Wróbel, S.; Gowda, B. T.; Haase, W. *J. Chem. Phys.* **1997**, *106*, 5904. (c) Szostak, M. M.; Wóicik, G.; Gallier, J.; Bertault, M.; Freundlich, P.; Kolodziej, A. H. *Chem. Phys.* **1998**, *229*, 275. (d) Jóźków, J.; Medycki, W.; Zaleski, J.; Jakubas, R.; Bator, G.; Ciunik, Z. *Phys. Chem. Chem. Phys.* **2001**, *3*, 3222. (e) Akutagawa, T.; Motokizawa, T.; Matsuura, K.; Nishihara, S.; Noro, S.; Nakamura, T. *J. Phys. Chem. B.* **2006**, *110*, 5897. (f) Horie, M.; Sassa, T.; Hashizume, D.; Suzuki, Y.; Osakada, K.; Wada, T. *Angew. Chem., Int. Ed.* **2007**, *46*, 4983.

(15) (a) Steimecke, G.; Sieler, H. J.; Krimse, R.; Hoyer, E. *Phosphorus Sulfur* **1979**, *7*, 49. (b) Nirgey, P. J. *Cryst. Growth* **1977**, *40*, 265.

Table 1. Crystal Data, Data Collection, and Reduction Parameter of Salts **1**−**4**

	1	**2**	**3**	**4**
chemical formula	$C_{32}H_{32}NO_6S_{10}Ni$	$C_{32}H_{44}NO_6S_{10}Ni$	$C_{36}H_{42}NO_6S_{10}Ni$	$C_{36}H_{54}NO_6S_{10}Ni$
fw	908.93	918.00	964.03	976.13
No.	*C*2/*c* (#15)	$P\bar{1}$ (#2)	*Cmcm* (#63)	$P2_1/n$ (#14)
a, Å	22.846(5)	12.396(6)	21.49(4)	13.770(3)
b, Å	8.0691(20)	12.624(5)	9.091(15)	15.988(4)
c, Å	21.662(4)	14.281(7)	22.55(4)	19.762(5)
α, deg		93.843(15)		
β, deg	101.702(5)	104.802(17)		92.027(8)
γ, deg		105.375(17)		
V, Å^3	3910.3(14)	2061.2(16)	4407(12)	4347.9(16)
Z	4	2	4	4
D_{calcd}, g·cm^{-1}	1.544	1.479	1.453	1.491
T	273	253	298	123
μ, cm^{-1}	10.73	10.19	9.57	9.71
reflns measured	18 381	19 926	20 156	41 918
independent reflns	4446	9259	2632	9935
reflns used	2518	5230	1583	6602
R [a]	0.143	0.043	0.038	0.036
$R_w(F^2)$ [a]	0.134	0.076	0.074	0.068
GOF	1.041	1.039	0.947	0.944

[a] $R = \Sigma||F_o| - |F_c||/\Sigma|F_o|$ and $R_w = (\Sigma\omega|F_o| - |F_c|)^2/\Sigma\omega F_o^2)^{1/2}$.

temperature. The reaction solvent was removed by reducing the pressure, then oil products were recrystallized from $CHCl_3$−hexane. White powder was precipitated, which was washed with cold ether (1.19 g) and recrystallized from $CHCl_3$−hexane (0.82 g). Elemental analysis. Calcd C: 50.24, H: 7.59, N: 5.86. Found. C: 50.10, H: 7.68, N: 5.65.

Preparation of Salts 1−4. The precursor monovalent (*n*-Bu_4N)[Ni(dmit)$_2$] salt was prepared according to the literature.[15a] The single crystals of salts **1**−**4** were obtained by the standard diffusion method in an *H*-shaped cell (∼50 mL).[15b] The green solution of (*n*-Bu_4N)[Ni(dmit)$_2$] (20 mg) in CH_3CN (∼20 mL) was poured into a solution of (Ph−NH_3^+)(BF_4^-) or (AD−NH_3^+)(BF_4^-) (∼60 mg) and DB[18]crown-6 or DCH[18]crown-6 (∼200 mg) in CH_3CN (∼30 mL) (detailed conditions of the single-crystal preparation are shown in Table S1 in the Supporting Information). After two weeks, single crystals (typical dimensions: 0.4 × 0.4 × 0.3 mm) were obtained as black blocks. The stoichiometry of crystals was determined by X-ray structural and elemental analyses (Table S2 in the Supporting Information).

Crystal Structure Determination. Crystallographic data (Table 1) were collected by a Rigaku RAXIS-RAPID diffractometer using Mo Kα ($\lambda = 0.71073$ Å) radiation from a graphite monochromator. Structure refinements were made using the full-matrix least-squares method on F^2. Calculations were performed using *Crystal Structure* software packages.[16] Parameters were refined using anisotropic temperature factors except for the hydrogen atom.

Calculations. The relative energy of the structures was calculated using the RHF/6−31(*d*) basis set.[17] The nearest-neighboring molecules around the phenyl ring of Ph−NH_3^+ and/or adamantyl group of AD−NH_3^+ were included in the calculations of the potential energy curves. The structural units of salts **1**, **2**, **3**, and **4** in the calculations were (Ph−NH_3^+)(DB[18]crown-6)[Ni(dmit)$_2$]$_2$, (Ph−NH_3^+)(DCH[18]crown-6)$_3$, (AD−NH_3^+)(DB[18]crown-6)[Ni(dmit)$_2$]$_2$, and (AD−NH_3^+)(DCH[18]crown-6)[Ni(dmit)$_2$]$_2$, respectively (Figures S5−S8 in the Supporting Information), which were different from the real stoichiometries of salts **1**−**4**. The atomic coordinates of salts **1**, **2**, and **4** based on the X-ray crystal structural analysis were used for the calculations. The potential energy curve could not be determined using the atomic coordinates of the X-ray structural analysis of salt **3** due to the orientational disorders of the AD−NH_3^+ cation. Thus, the geometry optimization of the disordered AD−NH_3^+ structure was first carried out by empirical PM3 calculation of salt **3**. The relative energy of the structures was obtained by evaluating the rigid rotation of phenyl and/or adamantyl units around the Ph−NH_3^+ and/or AD−NH_3^+ carbon−nitrogen bonds. Rotations were performed at every 30°, and the relative energies were calculated using fixed atomic coordinates. The transfer integrals (*t*) between the [Ni(dmit)$_2$]$^-$ anions were calculated within the tight-binding approximation using the extended Hückel molecular orbital method. The LUMO of the [Ni(dmit)$_2$]$^-$ molecule was used as the basis function.[18] Semiempirical parameters for Slater-type atomic orbitals were obtained from the literature.[18] The *t* values between each pair of molecules were assumed to be proportional to the overlap integral (*S*) via the equation $t = -10S$ eV.

Dielectric Measurements. Temperature-dependent dielectric constants were measured by the two-probe AC impedance method at the frequency of 100 × 10^3 Hz (HP4194A). A single crystal was placed into a cryogenic refrigerating system (Daikin PS24SS). The electrical contacts were prepared using gold paste (Tokuriki 8560) to attach the 10 μm A gold wires to the single crystal. The measurement axes of salts **1**, **2**, **3**, and **4** were perpendicular to the rotation axis of Ph−NH_3^+ and AD−NH_3^+ cations.

Solid-State ^{1}H NMR Measurements. Solid-state wide-line ^{1}H NMR spectra under static sample conditions were measured by solid

(16) (a) *Crystal Structure: Single Crystal Structure Analysis Software*, Ver. 3.6; Rigaku Corporation and Molecular Structure Corporation, 2004. (b) Sheldrick, G. M. *SHELX97 Programs for Crystal Structure Analysis*; Universitat Göttingen: Göttingen, Germany, 1998.

(17) Frisch, M. J.; Trucks, G. W.; Schlegel, H. B.; Scuseria, G. E.; Robb, M. A.; Cheeseman, J. R.; Montgomery, J. A., Jr.; Vreven, T.; Kudin, K. N.; Burant, J. C.; Millam, J. M.; Iyengar, S. S.; Tomasi, J.; Barone, V.; Mennucci, B.; Cossi, M.; Scalmani, G.; Rega, N.; Petersson, G. A.; Nakatsuji, H.; Hada, M.; Ehara, M.; Toyota, K.; Fukuda, R.; Hasegawa, J.; Ishida, M.; Nakajima, T.; Honda, Y.; Kitao, O.; Nakai, H.; Klene, M.; Li, X.; Knox, J. E.; Hratchian, H. P.; Cross, J. B.; Bakken, V.; Adamo, C.; Jaramillo, J.; Gomperts, R.; Stratmann, R. E.; Yazyev, O.; Austin, A. J.; Cammi, R.; Pomelli, C.; Ochterski, J. W.; Ayala, P. Y.; Morokuma, K.; Voth, G. A.; Salvador, P.; Dannenberg, J. J.; Zakrzewski, V. G.; Dapprich, S.; Daniels, A. D.; Strain, M. C.; Farkas, O.; Malick, D. K.; Rabuck, A. D.; Raghavachari, K.; Foresman, J. B.; Ortiz, J. V.; Cui, Q.; Baboul, A. G.; Clifford, S.; Cioslowski, J.; Stefanov, B. B.; Liu, G.; Liashenko, A.; Piskorz, P.; Komaromi, I.; Martin, R. L.; Fox, D. J.; Keith, T.; Al-Laham, M. A.; Peng, C. Y.; Nanayakkara, A.; Challacombe, M.; Gill, P. M. W.; Johnson, B.; Chen, W.; Wong, M. W.; Gonzalez, C.; Pople, J. A. *Gaussian 03*, Revision C.02; Gaussian, Inc.: Wallingford, CT, 2004.

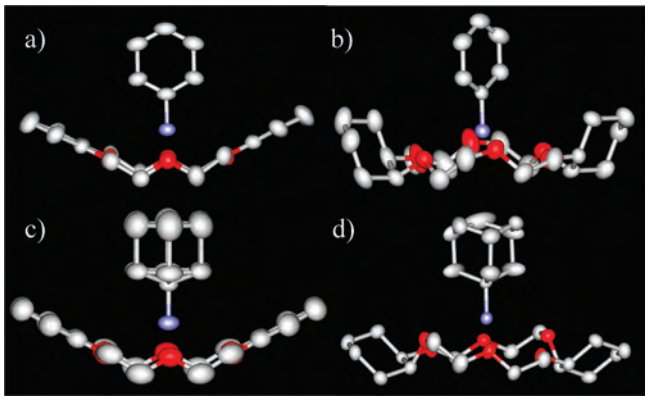

Figure 1. Supramolecular cation structures of (a) (Ph−NH_3^+)(DB[18]-crown-6) in salt **1**, (b) (Ph−NH_3^+)(DCH[18]crown-6) in salt **2**, (c) (AD−NH_3^+)(DB[18]crown-6) in salt **3**, and (d) (AD−NH_3^+)(DCH[18]crown-6) in salt **4** viewed parallel to the mean oxygen plane of [18]crown-6. Hydrogen atoms are omitted in the figures.

echo pulse sequence $^{\pi}/_{2_x} - \tau - {}^{\pi}/_{2_y}$ (the $^{\pi}/_2$ pulse width and τ were 1.3 and 10 μs, respectively) using a Bruker DSX 300 spectrometer with an operating frequency of 300 MHz for protons.

Magnetic Susceptibility. The temperature-dependent magnetic susceptibility and the magnetization magnetic field dependence were measured using a Quantum Design MPMS-XL5 SQUID magnetometer using polycrystalline samples. The applied magnetic field was 1 T for all temperature-dependent measurements.

Results and Discussion

Cation exchange reactions from (n-Bu_4N^+)[Ni(dmit)$_2$]$^-$ to Ph−NH_3^+ or AD−NH_3^+ in the presence of DB[18]crown-6 or DCH[18]crown-6 yielded monovalent [Ni(dmit)$_2$]$^-$ salts of(Ph−NH_3^+)(DB[18]crown-6)[Ni(dmit)$_2$]$^-$ (**1**),(Ph−NH_3^+)(DCH-[18]crown-6)[Ni(dmit)$_2$]$^-$ (**2**), (AD−NH_3^+)(DB[18]crown-6)[Ni(dmit)$_2$]$^-$ (**3**), and (AD−NH_3^+)(DCH[18]crown-6)[Ni(dmit)$_2$]$^-$ (**4**). The 1:1 adducts of supramolecular cations between organic ammonium and crown ether were constructed by six N−H$^+$∼O hydrogen bonds, forming a stand-up configuration of the C−N bond of phenyl and adamantyl groups with respect to the mean oxygen plane of DB[18]crown-6 or DCH[18]crown-6. Although the crystal symmetry of salt **3** (*C*/*mcm*) was higher than that of salt **1** (*C*2/c), isostructural cation and anion arrangements were observed in both crystals.

Cation Conformations. The structural flexibility of two dicyclohexyl rings in DCH[18]crown-6 was higher than that of two benzene rings in DB[18]crown-6, whereas the molecular surfaces of phenyl and adamantyl groups were constructed from π-electrons and sp^3 carbon−hydrogen bonds, respectively. These differences affected the supramolecular structure as well as intermolecular interactions between the cations and [Ni(dmit)$_2$]$^-$ anions. Figure 1 shows the supramolecular cation structures of salts **1**−**4** viewed along the mean oxygen plane of DB[18]crown-6 and DCH[18]crown-6. The 1:1 adducts between the organic ammoniums and crown ethers had similar stand up configuration of organic ammonium on bulky crown ethers.

A half (Ph−NH_3^+)(DB[18]crown6) and a quarter (AD-NH_3^+)(DB[18]crown-6) were the crystallographically independent supramolecular cation units in salts **1** and **3**. The DB[18]crown-6 in salts **1** and **3** had a jackknife-type conformation, where the folding angles between two benzene rings were 128.4 and 123.4°, respectively (parts a and c of Figure 1). The C−N bonds of Ph−NH_3^+ and AD−NH_3^+ in salts **1**−**4** were almost perpendicular to the mean oxygen planes of crown ethers. Average hydrogen-bonding N∼O distances between the nitrogen and oxygen atoms of salts **1** and **3** were 2.97 and 2.98 Å, respectively, which were comparable to the standard N−H$^+$∼O hydrogen bond length.[19] Although the jackknife conformations of DB[18]crown-6 in salts **1** and **3** were similar (parts a and c of Figure 1), the magnitude of the thermal fluctuation and orientation of ammonium cations were quite different. The orientational disorder of AD−NH_3^+ was observed in salt **3** (section of packing structure), which was intrinsic because the same disorder arrangement was confirmed in structural analyses with low crystal symmetry of *C*2 (full AD−NH_3^+ was the crystallographically independent unit, as seen in Figures S9 and S10 in the Supporting Information).

The conformations of DCH[18]crown-6 in salts **2** and **4** were slightly different. Two cyclohexane rings in salt **2** adopted the jackknife-like conformation, whereas those in salt **4** were almost parallel to each other. The (Ph−NH_3^+)(DCH-[18]crown-6) and (AD−NH_3^+)(DCH[18]crown-6) units were both crystallographically independent, indicating the non-centrosymmetrical supramolecular cation structure of salts **2** and **4**. The average hydrogen bonding Ñ–O distances in salts **2** and **4** were 2.92 and 3.02 Å, respectively, which were almost the same as those in salts **1** and **3**. The supramolecular cation structures of salts **1**−**4** were constructed from the standard N−H$^+$∼O hydrogen bonding interactions.[19] The adamantyl group of salt **4** had a C_{3v} symmetry without orientational disorder, suggesting a 120° rotational symmetry. The similar supramolecular cation structures of (Ph−NH_3^+)(DB-[18]crown-6) and (AD−NH_3^+)(DB[18]crown-6) yielded isostructural [Ni(dmit)$_2$]$^-$ arrangements in salts **1** and **3**, whereas the slight conformational difference between cyclohexane rings in salts **2** and **4** led to the different [Ni(dmit)$_2$]$^-$ arrangements and magnetic behaviors (sections of packing structure and magnetic properties).

Packing Structures of Cations and [Ni(dmit)$_2$]$^-$ Anions. Each [Ni(dmit)$_2$]$^-$ anion had one $S = {}^1/_2$ spin, and the arrangement of [Ni(dmit)$_2$]$^-$ anions directly determined the magnetism. Transfer integrals based on extended Hückel molecular orbital calculations were used to evaluate the magnitude of the intermolecular interactions between [Ni(dmit)$_2$]$^-$ anions within the crystals.[20] The magnetic exchange energy (J) is proportional to the square of the transfer integral, $J \sim 4t^2/U_{\text{eff}}$, where U_{eff} is the effective on-site

(18) Mori, T.; Kobayashi, A.; Sasaki, Y.; Kobayashi, H.; Saito, G.; Inokuchi, H. *Bull. Chem. Soc. Jpn.* **1984**, *57*, 627.

(19) (a) Jeffrey, G. A. *An Introduction to Hydrogen Bonding*; Truhlar, D. G., Ed.; Oxford University Press: New York, 1997. (b) Pimentel, G. C.; McClellan, A. L. *The Hydrogen Bond*; Freemann: San Francisco, 1960. (c) Hamilton, W. C.; Ibers, J. A. *Hydrogen Bonding in Solids*; Breslow, R.; Karplus, M., Eds.; Benjamin Inc: New York, 1968.

(20) (a) Scott, J. C. *Semiconductor and Semimetals. Highly Conducting Quasi-One-Dimensional Organic Crystals*; Conwell, E. Ed.; Academic Press: New York, 1988, 385. (b) Carlin, R. L. *Magnetochemistry*; Springer-Verlag: Heidelberg, 1986. (c) Kahn, O. *Molecular Magnetism*; VCH: New York, 1993.

Table 2. Transfer Integrals (t) and Magnetic Parameters of Salts **1**−**4**

	1	**2**	**3**	**4**
t_1, meV[a]	14.2	1.7	9.12	4.09
t_2, meV[a]	2.0	−1.6		−0.76
$[Ni(dmit)_2]^-$ arrangement	2D	1D	2D	1D
g (298 K)[b]	2.04622	2.03943	2.06135	2.04599
ΔH (298 K), mT[b]	0.46	2.78	1.54	6.00
C, emu K mol^{-1}	0.38	0.39	0.37	0.39
θ or J/k_B, K	−1.3	+0.9	−0.4	−39.5
magnetism[c]	C−W[c]	C−W[c]	C−W[c]	S−T[c]

[a] The transfer integrals (t) were obtained by the LUMO of $[Ni(dmit)_2]^-$ based on the extended Hückel calculation ($t = -10S$ eV, where S is the overlap integral). [b] The g value (g) and line-width (ΔH) of the $[Ni(dmit)_2]^-$ anion were determined from the electron spin resonance spectra for single crystals at 298 K. [c] S−T and C−W are the singlet−triplet thermal excitation and Curie−Weiss models, respectively.

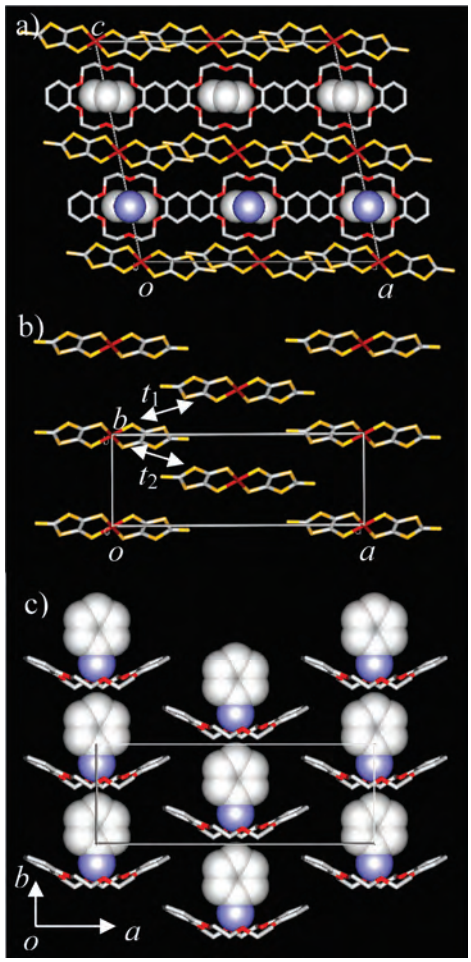

Figure 2. Crystal structures of salt **1**. (a) Unit cell viewed along the b axis. Ph−NH_3^+ cations without hydrogen atoms were drawn by CPK representation. (b) $[Ni(dmit)_2]^-$ anion arrangement within the ab plane. Two kinds of intermolecular interactions (t_1 and t_2) were observed along the $a + b-$ and $-a + b$ axes, respectively. (c) (Ph−NH_3^+)(DB[18]crown-6) cation arrangement within the ab plane viewed along the c axis.

Coulomb repulsive energy in the solid.[20] Table 2 summarizes the transfer integrals and magnetic parameters of salts **1**−**4**.

Part a of Figure 2 shows the unit cell of salt **1** viewed along the b axis. The $[Ni(dmit)_2]^-$ anion arrangement in the ac plane yielded the 2D intermolecular interactions $t_1 = 14.2$ meV and $t_2 = 2.0$ meV (part b of Figure 2). An alternate arrangement of cation and anion layers was elongated along the c axis (parts b and c of Figure 2), which isolated each 2D $[Ni(dmit)_2]^-$ layer. In salt **1**, the lateral sulfur atoms of two nearest-neighboring $[Ni(dmit)_2]^-$ anions interacted with the π plane of Ph−NH_3^+, which prevented the rotation of the phenyl ring with 2-fold 180° flip-flop motion. The uniform stack of jackknife-shaped (Ph−NH_3^+)(DB[18]crown-6) cations arranged the direction of dipole moments of Ph−NH_3^+ cations within the ab plane (part c of Figure 2). However, the total dipole moment canceled out due to the inverted dipole arrangement of cation layers along the c axis. Although sufficient crystalline void space was achieved for the phenyl ring along the a axis, molecular rotation was rather restricted by the effective intermolecular interactions between the π plane of Ph−NH_3^+ and lateral sulfur atoms of the two nearest-neighboring $[Ni(dmit)_2]^-$ anions along the c axis (part a of Figure S14).

The crystal structure of salt **3** was isomorphous to that of salt **1**, where the alternate cation and anion layer arrangement was observed along the c axis, as shown in part a of Figure 2. Because of the higher crystal symmetry of salt **3** ($Cmcm$) as compared to that of salt **1** ($C2/c$), one intermolecular interaction ($t_1 = t_2 = 9.12$ meV) was observed in the ab plane (part b of Figure 2). In the cation layer, an average structure of two kinds of molecular orientations (**I** and **II** in part b of Figure 3), where orientation **II** was generated by a 60° rotation from orientation **I** around the C−N bond of AD−NH_3^+, was confirmed in the X-ray crystal structural analysis (parts a and b of Figure 3). The rotation of the adamantyl group was affected by the intermolecular interactions between the lateral sulfur atoms of the $[Ni(dmit)_2]^-$ anions along the c axis. The isotropic molecular structure of AD−NH_3^+ was effective in constructing the space for molecular rotation in the crystal. Sufficient crystalline space for the adamantyl ring was achieved, although the molecular rotation was somewhat restricted by the intermolecular interactions between the AD−NH_3^+ and lateral sulfur atoms of the two nearest-neighboring $[Ni(dmit)_2]^-$ anions along the c axis (part b of Figure S14). It should be noted that the rotation of the NH_3^+ moiety around the C−N bond of AD−NH_3^+ was also expected to occur in the solid state. Because the magnitude of the potential barrier for the rotation of NH_3^+ moiety was less than ~2 kJmol^{-1},[8d] the rotation of the $-NH_3^+$ moiety was negligible in comparison with that of the adamantyl group in salt **3**.

The packing structure of cations and anions in salt **2** was different from those of salts **1** and **3**. Parts a and b of Figure 4 show the unit cells of salt **2** viewed along the a and c axes, respectively. The alternate cation and anion layers within the ac plane were arranged along the b axis. In the anion layer, two kinds of lateral sulfur−sulfur intermolecular interactions between the $[Ni(dmit)_2]^-$ anions ($t_1 = 1.7$ and $t_2 = -1.6$ meV) were elongated along the a axis. Almost the same magnitude of t_1 and t_2 interactions formed a uniform 1D chain. Along the c axis, the shortest sulfur−sulfur distance between the $[Ni(dmit)_2]^-$ anions (5.931 Å) was far from the effective intermolecular interaction. The supramolecular cations were arranged within the ac plane, where the dipole moments of Ph−NH_3^+ cations were arranged in antiparallel manner with respect to each other (part a of Figure 4). The π plane of the Ph−NH_3^+ cation was

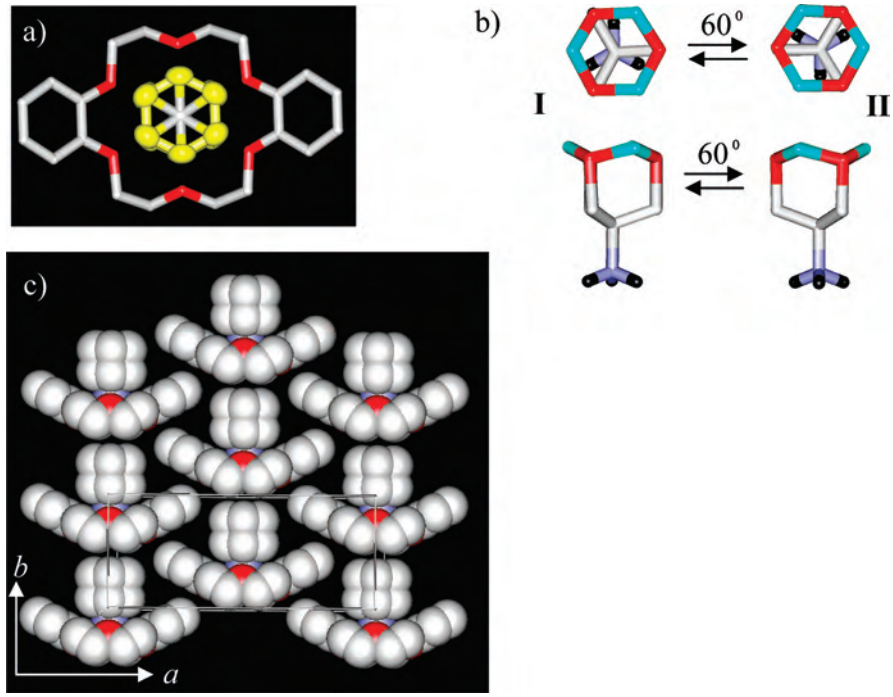

Figure 3. Supramolecular cation structure of (AD−NH_3^+)(DB[18]crown-6) in salt **3** ($T = 298$ K). (a) Orientational disorder of the adamantyl group (yellow-colored thermal ellipsoid) viewed along the C−N bond of AD-NH_3^+. (b) Two kinds of orientations (**I** and **II**) rotated by 60° with respect to each other. An average structure of orientations **I** and **II** yielded the cation structure. (c) 2D layer of (AD−NH_3^+)(DB[18]crown-6) cations within the *ab* plane (CPK representation).

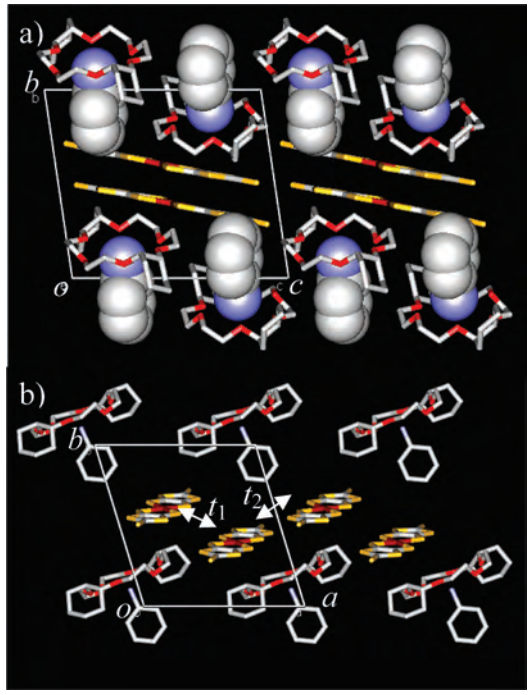

Figure 4. Crystal structure of salt **2**. Unit cell viewed along the (a) *a* axis and (b) *c* axis. Two intermolecular interactions (t_1 and t_2) were observed along the *a* axis. Hydrogen atoms are omitted in the figure.

surrounded by the two nearest-neighboring DCH[18]crown-6 molecules along the *c* axis, which prevented the rotation of Ph−NH_3^+ (part c of Figure S14 in the Supporting Information). No effective intermolecular interaction was observed between the π plane of Ph−NH_3^+ and $[Ni(dmit)_2]^-$ along the *b* axis.

Parts a and b of Figure 5 show the unit cell of salt **4** viewed along the *a* and *b* axes, respectively. The 1D intermolecular interaction through the lateral sulfur−sulfur contacts between $[Ni(dmit)_2]^-$ anions was observed along the *a* axis. Because the magnitude of the t_1 interaction (4.09 meV) was about five times larger than that of the t_2 interaction (−0.76 meV), the lateral $[Ni(dmit)_2]^-$ dimer was arranged along the *a* axis as a result of the weak t_2 interactions (part b of Figure 5). The 1D cation arrangement was also observed along the *a* axis, where the alternate dipole arrangement of AD−NH_3^+ cations canceled the net dipole moment. Because the intermolecular interactions between $[Ni(dmit)_2]^-$ anions were not observed along the *b* and *c* axes, the lateral $[Ni(dmit)_2]^-$ chains were isolated from each other. The relatively flat conformation of the two cyclohexane rings of (DCH[18]crown-6 in (AD-NH_3^+)(DCH[18]crown-6) (part d of Figure 1) did not affect the rotation of the AD−NH_3^+ cation because of reduction of the steric repulsion between cyclohexane rings and the adamantyl group. Around the AD−NH_3^+ cation, the weakly interacting terminal sulfur atoms of $[Ni(dmit)_2]^-$ anions affected the rotation of AD−NH_3^+ (part d of Figure S14 in the Supporting Information).

Potential Energy of Cation Rotations. The rotation mode and frequency of phenyl and adamantyl groups in the solid state were determined by the potential energy curve and the magnitude of the potential energy barrier (ΔE). The potential energy curves of the molecular rotation of phenyl and adamantyl groups in salts **1**, **2**, **3**, and **4** were calculated using the RHF/6−31(*d*) basis set.[17] Beside the supramolecular

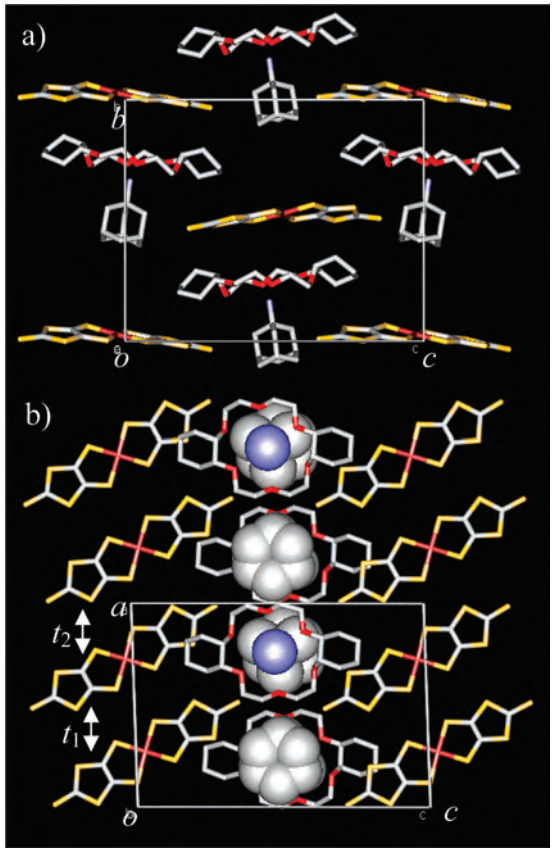

Figure 5. Crystal structure of salt **4**. Unit cell viewed along the (a) *a* and (b) *b* axes. Alternate cation and cation layers were elongated along the *c* axis. The AD−NH_3^+ cations without the hydrogen atoms in part b of Figure 5 were drawn by CPK representation. Two intermolecular interactions (t_1 and t_2) were observed between the $[Ni(dmit)_2]^-$ anions along the *a* axis.

cation, the nearest-neighboring molecules of $[Ni(dmit)_2]^-$ or crown ethers were included in the calculations (Figures S5−S8 in the Supporting Information). The relative energies as a function of the rotational angle ϕ around the C−N bond of Ph−NH_3^+ and AD−NH_3^+ were determined at every 30° rotation.

Part a of Figure 6 shows the rotational angle dependence of the relative energy (ΔE) of (Ph−NH_3^+)(DB[18]crown-6)$[Ni(dmit)_2]_2$ and (Ph−NH_3^+)(DCH[18]crown-6)$_3$ in salts **1** and **2**, where the relative energy at $\phi = 0°$ is defined as zero. For the rotational angle ϕ, the initial atomic coordinates from the X-ray crystal structural analysis corresponded to the first potential energy minimum at $\phi = 0°$, whereas the second potential energy minimum was observed around $\phi = 180°$. The double-minimum potential with two stable molecular orientations suggested a 180° flip-flop motion of the phenyl ring in salts **1** and **2**, which is consistent with that in (Ph−NH_3^+)([18]crown-6)$[Ni(dmit)_2]^-$.[8d] The fact that only one position was observed for the phenyl ring in the crystal structural analysis presumably indicates the 180° periodicity of the potential-energy curve. The magnitude of ΔE of salt **2** (∼340 kJmol^{-1}) was about twice that of salt **1** (∼180 kJmol^{-1}), suggesting that the rotation of Ph−NH_3^+ in salt **2** was much hindered to the presence of the two nearest-neighboring DCH[18]crown-6. The ΔE in salt **1** (∼180 kJmol^{-1}) was larger than that in (Ph−NH_3^+)([18]crown-6)$[Ni(dmit)_2]^-$ (i.e., 40 kJmol^{-1}), where the symmetrical 180° flip-flop motion of Ph−NH_3^+ with a flip-flop frequency of ∼10^6 Hz was confirmed at room temperature.[8d]

The rotational angle dependence of ΔE for the structural unit of (AD−NH_3^+)(DB[18]crown-6)$[Ni(dmit)_2]_2$ and (AD−NH_3^+)(DCH[18]crown-6)$[Ni(dmit)_2]_2$ in salts **3** and **4** were different from those in salts **1** and **2** from the viewpoints of rotational symmetry and potential-energy barrier height. For rotational angle ϕ, the initial atomic coordinates from the X-ray crystal structural analysis corresponded to the first potential energy minimum at $\phi = 0°$, whereas the second and third potential-energy minima were observed at around $\phi = 120°$ and $\phi = 240°$, respectively. The triple minimum potential energy curve suggested the 120° rotation of the adamantyl group. The one orientation of the adamantyl group in the X-ray crystal structural analysis of salt **4** was consistent with the 120° periodicity in the calculation of the potential energy curve. Because the magnitude of ΔE in salt **4** (∼15 kJmol^{-1}) was 1 order of magnitude smaller than that of salt **1** (∼180 kJmol^{-1}), the 120° rapid rotation of the adamantyl group is expected to occur at room temperature. The orientational disorder of the adamantyl group in salt **3** was prevented to determine the potential energy curve, thus, the optimized molecular structure of the adamantyl group in the (AD−NH_3^+)(DB[18]crown-6)$[Ni(dmit)_2]_2$ structure was used for the calculation. The triple minimum potential energy curve with a ΔE of ∼18 kJmol^{-1} was similar to those of salt **3**, suggesting rapid rotation of the adamantyl group at room temperature. It should be noted that the symmetry breaking of the potential energy curve was assumed in salt **4** due to an asymmetrical intermolecular interaction between the adamantyl group and two cyclohexane rings of *meso*-DCH[18]crown-6.

Extremely low potential-energy barriers for the rotation of the adamantyl group were achieved in salts **3** (ΔE ∼18 kJmol^{-1}) and **4** (ΔE ∼15 kJmol^{-1}), which were comparable to those of ethane (ΔE ∼12 kJmol^{-1}) and butane (ΔE = 17−25 kJmol^{-1}) for rotation around the C−C single bond.[21] The potential-energy barriers for rotation around the C−C bond of ethane and butane are dominated by the steric hindrance and hyperconjugation effects, whereas the ΔE of salts **3** and **4** were determined by the steric hindrance of the intermolecular S̃–H interaction between $[Ni(dmit)_2]$ and AD−NH_3^+. In the plastic crystalline state, the rotation of adamantane (and cyclohexane) has been examined by temperature-dependent solid-state ^{1}H NMR spectra. The activation energy for the rotation of adamantane (and cyclohexane), which keeps its center of gravity during the rotation, was 12.9 kJmol^{-1} (and 6.4 kJmol^{-1}, respectively).[22] This is almost similar to the potential energy barriers of salts **3** and **4**, suggesting the similar rotation of the adamantyl group in

(21) (a) Eyring, H.; Grant, D. M.; Hecht, H. *J. Chem. Educ.* **1962**, *39*, 466. (b) Lowe, J. P. *Science* **1973**, *179*, 527. (c) Verma, A. L.; Murphy, W. F.; Bernstein, H. J. *J. Chem. Phys.* **1974**, *60*, 1540. (d) Pophristic, V.; Goodman, L. *Nature* **2001**, *411*, 565. (e) Mo, Y.; Gao, J. *Acc. Chem. Res.* **2007**, *40*, 113.

(22) (a) Resing, H. A. *Mol. Cryst. Liq. Cryst.* **1969**, *9*, 101. (b) O'Reilly, D. E.; Peterson, E. M.; Hogenboom, D. L. *J. Chem. Phys.* **1972**, *57*, 3969.

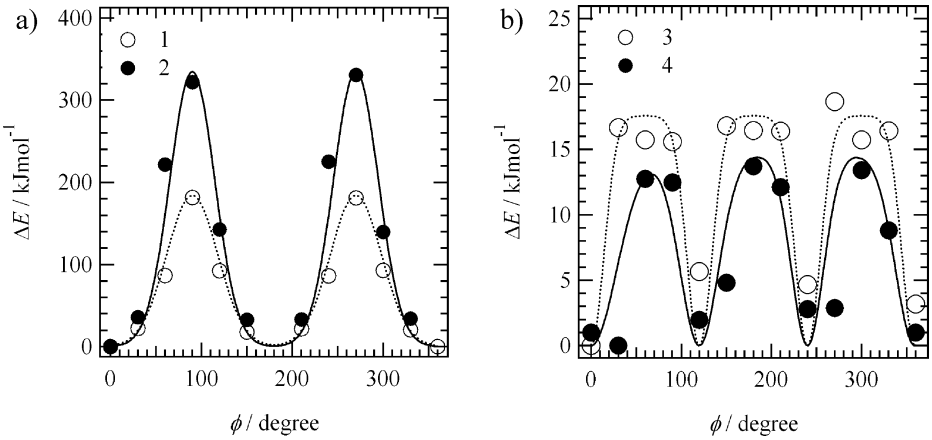

Figure 6. Potential-energy curves of phenyl and adamantyl group rotations in the cation structures. The rotations of (a) the phenyl group around the C−N bond of Ph−NH_3^+ in salts **1** and **2** and of (b) the adamantyl group in salts **3** and **4**. The structural units for the calculations of salts **1**, **2**, **3**, and **4** were (Ph−NH_3^+)(DB[18]crown-6)[Ni(dmit)$_2$]$_2$, (Ph−NH_3^+)(DCH[18]crown-6)$_3$, (AD−NH_3^+)(DB[18]crown-6)[Ni(dmit)$_2$]$_2$, and (AD−NH_3^+)(DCH[18]crown-6)[Ni(dmit)$_2$]$_2$, respectively. The solid and dashed lines are guides for the eye.

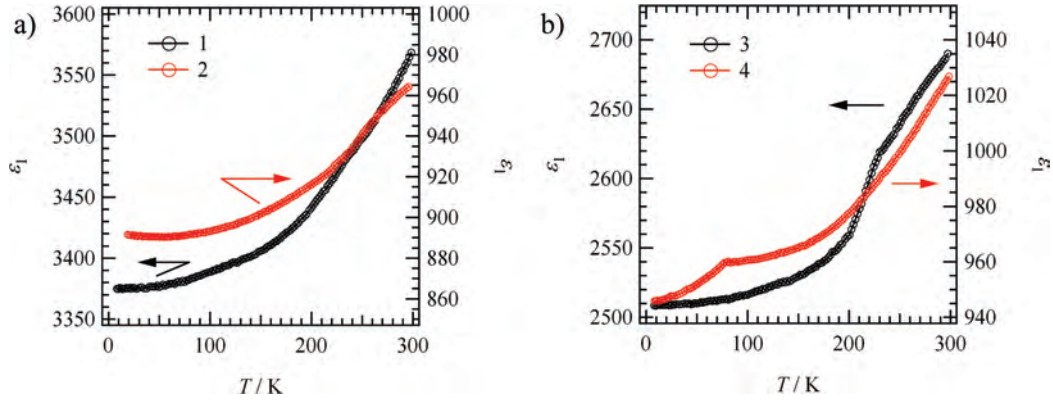

Figure 7. Temperature-dependent dielectric constants (ϵ_1) of salts (a) **1** and **2**, and (b) **3** and **4**. The measurement frequency was fixed at 100 kHz. The electric field was applied perpendicular to the rotation axis of the Ph−NH_3^+ and AD−NH_3^+ cations.

salts **3** and **4** in comparison with the plastic crystalline state of adamantane. An extremely low activation energy for molecular rotation has been reported for the C_{60} crystal (ΔE ~6 kJmol^{-1}) at 298 K,[23] which is almost equal to those of salts **3** and **4**. The suitable size and shape of the adamantyl group with respect to the space created by DB[18]crown-6 and DCH[18]crown-6 is presumably one reason for the low potential-energy barrier. Another possible reason for the low potential energy barrier of the adamantyl group in salts **3** and **4** is the rigid framework of the crystal. Because the crystal lattice of salts **3** and **4** was mainly constructed by the electrostatic Coulomb interaction between the anionic [Ni(dmit)$_2$]$^-$ and cationic −NH_3^+ group of AD−NH_3^+, the crystalline rotation space of the adamantyl group in salts **3** and **4** was kept within the rigid framework of the crystals.

Dielectric Properties. Temperature-dependent dielectric constants (ϵ_1) of salts **1**−**4** were evaluated to obtain information on the molecular motions.[24] Figure 7 plots ϵ_1 vs T for salts **1**−**4** at a measurement frequency (f) of 100 kHz. The electric field was applied perpendicular direction to the rotation axis of the Ph−NH_3^+ and AD−NH_3^+ cations. The thermally activated molecular rotations of the cations affect the dielectric response when the temperature is lowered. When the rotation frequency of the rotator was almost equal to the measurement frequency (f = 100 kHz), a great enhancement in the dielectric response appeared in the ϵ_1 versus T plots.[24] The structural fluctuation of the cations enhanced the magnitude of ϵ_1, which was suppressed by lowering the temperature owing to the reduced thermal motion at lower temperatures. Because the room-temperature ϵ_1 of salts **1** and **3** (~3000) was larger than those of salts **2** and **4** (~1000), the introduction of DB[18]crown-6 molecules has a tendency to enhance the magnitude of ϵ_1 relative to that of DCH[18]crown-6. A gradual enhancement of ϵ_1 without an anomaly was observed in salts **1** and **2** upon increasing the temperatures to 300 K, whereas anomalies of ϵ_1 were observed in salts **3** and **4** at around 230 and 80 K, respectively.

From the isomorphous crystal structures of salts **1** and **3**, the phenyl and adamantyl groups were expected to have similar crystalline rotation environments. However, the potential energy barrier for the rotation of the adamantyl group in salt **3** (ΔE ~18 kJmol^{-1}) was 1 order of magnitude lower than that of the phenyl group in salt **1** (ΔE ~180

(23) (a) Tycko, R.; Dabbagh, G.; Fleming, R. M.; Haddon, R. C.; Makhija, A. V.; Zahurak, S. M. *Phys. Rev. Lett.* **1991**, *67*, 1886. (b) Johnson, R. D.; Bethune, D. S.; Yannoni, C. S. *Acc. Chem. Res.* **1992**, *25*, 169. (c) Johnson, R. D.; Yannoni, C. S.; Dorn, H. C.; Salem, J. R.; Bethune, D. S. *Science* **1992**, *255*, 1235.

(24) Kao, K. C. *Dielectric Phenomena in Solids*; Elsevier: Amsterdam, 2004.

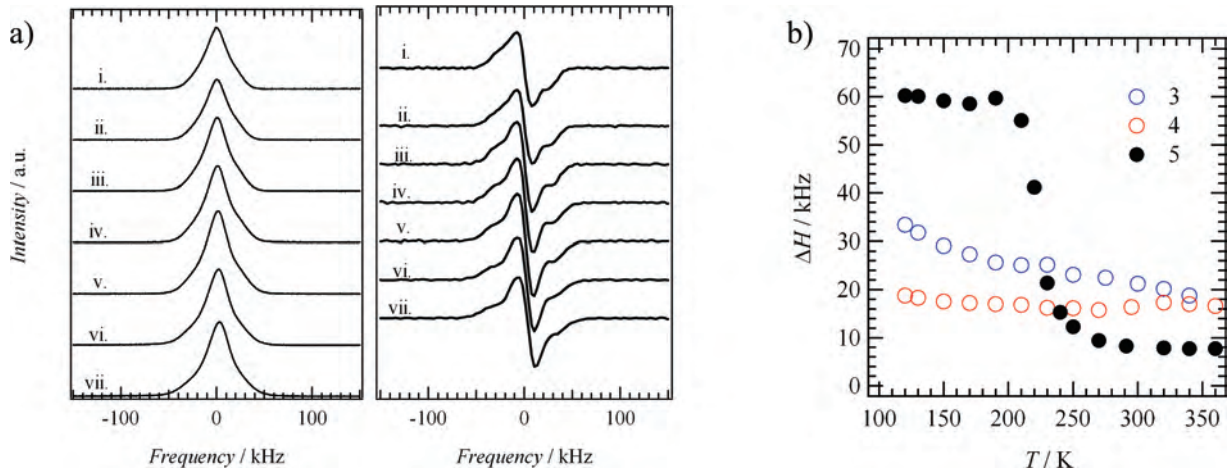

Figure 8. Temperature-dependent solid-state wide-line ^{1}H NMR spectra of salt **3**. (a) Spectral changes (left) and the first derivative of the spectra (right) obtained by decreasing the temperatures from (i) 360 K, (ii) 320 K, (iii) 270 K, (iv) 230 K, (v) 190 K, (vi) 150 K to (vii) 120 K. (b) Temperature-dependent line-width (ΔH_A) of salts **3** and **4** along with that of $Cs^+_2([18]crown\text{-}6)_3[Ni(dmit)_2]_2$ (**5**).

kJmol^{-1}), owing to the loose molecular packing and isotropic molecular structure of the adamantyl group. In fact, a dielectric anomaly was observed at around ~230 K in salt **3**. A notable structural difference between salts **1** and **3** was assumed to be the packing structure of cations, suggesting that the ϵ_1 anomaly around 230 K of salt **3** was related to a changing of the rotational freedom of the adamantyl group induced by lowering of the temperature. In salt **1**, the molecular rotation of the phenyl ring was ignored within the limit of measuring frequencies and temperatures. Because the height of ΔE for salt **2** (~340 kJmol^{-1}) was almost twice that of salt **1**, the rotation of the phenyl ring in salt **2** is restricted at room temperature. Thus, no anomaly appeared in the temperature-dependent dielectric properties of salt **2**. On the other hand, the ΔE of salts **3** (~18 kJmol^{-1}) and **4** (~15 kJmol^{-1}) was almost on the order of the thermal energy at room temperature ($k_BT \approx 2.5$ kJmol^{-1}), assuming a rapid rotation of the adamantyl group at room temperature. However, lowering of the temperature resulted in a decrease in the rotation frequency of the adamantyl group in salts **3** and **4**, which became comparable to the measurement frequency (100 kHz) at 80 and 230 K, respectively.

Solid-State ^{1}H NMR of Salts 3 and 4. On the basis of the crystal structures, ab initio calculations, and dielectric properties, salts **3** and **4** were assumed to contain the crystalline rotator of the adamantyl group. The temperature-dependent solid-state wide-line ^{1}H NMR spectra of salts **3** and **4** were evaluated to confirm the rotations of the adamantyl group. Part a of Figure 8 shows the temperature-dependent spectral changes (left figure) and the first derivative (right figure) of the wide line ^{1}H NMR spectra of salt **3**.

Because the rotation of bulky DB[18]crown-6 and DCH[18]crown-6 should be suppressed in salts **3** and **4**, the rotations of the adamantyl group contributed to the temperature-dependent spectral changes in the wide-line ^{1}H NMR spectra. In salt **3**, 18 protons of AD$-NH_3^+$ and 32 protons of DB[18]crown-6 were overlapped in the ^{1}H NMR spectrum. The 18 protons showed a temperature-dependent behavior, whereas the behavior of the 32 protons was almost independent of temperature. Because a distinct temperature-dependent spectral change in the line-width of the ^{1}H NMR spectra of salt **3** could not be seen in the left figure in part a of Figure 8, the first derivative of the spectrum was employed to distinguish between the line-width components of AD$-NH_3^+$ (ΔH_A: narrow line-width component) and DB[18]crown-6 (ΔH_B: wide line-width component). The peak-to-peak line width of the wide-line-width component (DB[18]crown-6) was ~65 kHz and was almost temperature-independent, which was consistent with that of the frozen [18]crown-6 (60 kHz) in the crytsal.[8a] In $(Cs^+)_2([18]crown\text{-}6)_3[Ni(dmit)_2]_2$ (**5**), the rotation of [18]crown-6 was frozen at around 220 K upon decreasing the temperature, where a dramatic change in line width was observed from ~10 kHz (motional state) to ~60 kHz (freeze state).[8a] The negligible motion of protons in DB[18]crown-6 from 120 to 360 K resulted in a temperature-independent line-width of ~60 KHz in salt **3**.

The temperature-dependent narrow line width (ΔH_A) was assigned to the protons of AD$-NH_3^+$ in salt **3**. Increasing the temperature slightly increased the ΔH_A of salt **3** from 20 kHz ($T = 350$ K) to 30 kHz ($T = 120$ K). A discontinuous increase in ΔH_A was confirmed at around 250 K, which was almost where the consistent ϵ_1 anomaly appeared. The temperature-dependent line-width of salt **4** was basically similar to that of salt **3**, where two kinds of temperature-independent line-widths (ΔH_A and ΔH_B) were observed over the temperature range studied. The nearly temperature-independent line widths ΔH_A and ΔH_B were observed at ~20 and ~65 kHz, respectively. Because the dielectric peak of salt **4** was observed at ~80 K, the rotation frequency of the adamantyl group over the temperature range from 360 to 120 K in the ^{1}H NMR spectra was faster than the measurement frequency of dielectric behavior ($f = 100$ kHz). Assuming the dielectric peak in salt **4** arose from the rotation of the adamantyl group, the rotation frequency of the adamantyl group was estimated to be around 100 kHz at 80 K. Thus, the spectral change in the temperature-dependent ^{1}H NMR spectra was not observed due to the change in the rotational frequency of the adamantyl group.

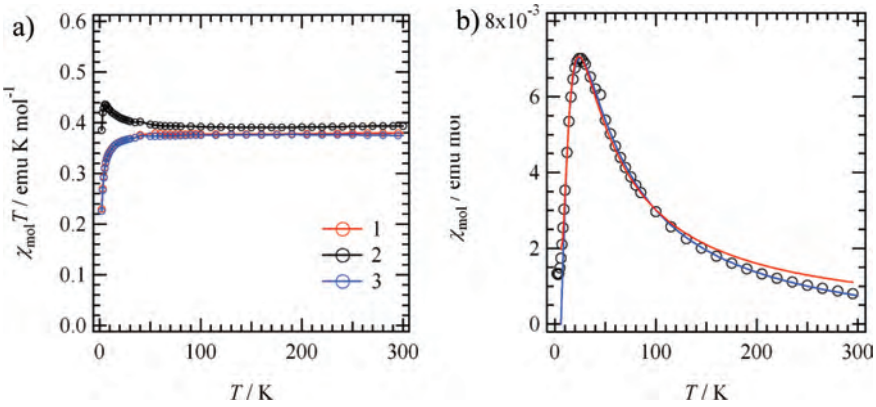

Figure 9. Temperature-dependent magnetic susceptibility of salts **1**−**4**. (a) $\chi_{mol}T$ vs T plots of salts **1** (red), **2** (black), and **3** (blue) per $[Ni(dmit)_2]^-$ anion. (b) χ_{mol} vs T plots for salt **4** per $[Ni(dmit)_2]^-$. The blue and red lines represent the fits obtained using the 1D alternate antiferromagnetic Heisenberg model and singlet−triplet thermal excitation model, respectively (text).

Magnetic Properties. The temperature-dependent molar magnetic susceptibility (χ_{mol}) per $[Ni(dmit)_2]^-$ anion was directly affected by the anion arrangements in the crystals. Part a of Figure 9 plots $\chi_{mol}T$ versus T for salts **1**, **2**, and **3**. In salts **1** and **3**, 2D intermolecular interactions in the $[Ni(dmit)_2]^-$ layers were observed within the magnitude of transfer integrals below 15 meV, which led to a weak antiferromagnetic interaction between $[Ni(dmit)_2]^-$ anions. The χ_{mol} versus T plots for salts **1** and **3** exhibited typical Curie−Weiss behavior with a Weiss temperature (θ) of −1.3 and −0.4 K, respectively (Table 2).[20] The magnetic spins on the $[Ni(dmit)_2]^-$ anion within the 2D layer of salts **1** and **3** were almost identical to each other.

Although similar 1D lateral intermolecular interactions through the sulfur−sulfur contacts between the $[Ni(dmit)_2]^-$ anions were observed in salts **2** and **4**, the magnetic exchange interactions of salts **2** and **4** were ferromagnetic and antiferromagnetic, respectively. Although constant $\chi_{mol}T$ values were observed in salt **2** above 30 K, an enhancement in the $\chi_{mol}T$ value was found below 30 K. A ferromagnetic interaction with a Weiss temperature of $\theta = +0.9$ K was observed at low temperatures ($T < 30$ K). The ferromagnetic ordering could not be confirmed by the magnetization − magnetic field ($M - H$) and AC susceptibility measurements. The $M - H$ curve ($-5\ T < M < +5$ T) at 2 K showed a nonlinear behavior with a saturation of M to ∼1.73 μ_B at 5 T (Figure S15 in the Supporting Information). On the other hand, the θ_{mol} versus T behavior of salt **4** clearly showed the antiferromagnetic interaction between the $[Ni(dmit)_2]^-$ anions (part b of Figure 9). The χ_{mol} versus T plots around room temperature exhibited Curie−Weiss behavior. Further lowering of the temperature resulted in a broad χ_{mol} maximum around 25 K, and a rapid decrease in χ_{mol} was observed below 25 K. This kind of temperature dependence has been typically observed in the 1D antiferromagnetic Heisenberg chain or singlet−triplet dimer. The magnitude of intrachain transfer integrals ($t_1 = 4.09$ meV and $t_2 = 0.76$ meV) of salt **4** suggested the formation of an alternate 1D chain or isolated lateral $[Ni(dmit)_2]^-$ dimer, which depended on the ratio of intra- (J_1) to interdimer magnetic exchange energy (J_2). Assuming the relationship $J \sim t^2$, the J_1/J_2 ratio based on the transfer integrals of salt **4** was about 30 (intradimer $J_1 \gg$ interdimer J_2). First, we applied the alternate antiferromagnetic Heisenberg model for the χ_{mol} versus T behavior of salt **4**,[25] which almost reproduced the temperature-dependent magnetic behavior using the fitting parameters' intradimer $J_1 = -20$ K and interdimer $J_2 = -7.4$ K. However, the J_1/J_2 ratio of ∼3:1 was inconsistent with the ratio from the calculation. Thus, we used the singlet−triplet (S−T) thermal excitation model.[20c] Although a slight deviation from the theoretical model was observed above 150 K, the χ_{mol} versus T behavior of salt **4** was in good agreement with this theoretical model. From the crystal structure, theoretical calculations, and fitting results of magnetic susceptibility, the magnetic properties of salt **4** could be explained by the lateral $[Ni(dmit)_2]^-$ dimer.

Although 1D $[Ni(dmit)_2]^-$ anion arrangements were observed in salts **2** and **4** (Figure S16 in the Supporting Information), different magnetic interactions appeared as ferromagnetic and antiferromagnetic interactions. The $[Ni(dmit)_2]^-$ anions of salt **2** were arranged in the up and down configurations with almost equal t_1 and t_2 interactions, whereas those of salt **4** were constructed from a nonuniform $[Ni(dmit)_2]^-$ dimer arrangement with $t_1 \gg t_2$ interactions. Another notable structural difference was observed in the largely deformed conformation of the $[Ni(dmit)_2]^-$ anion in salt **4**. The uniform 1D chain along the long axis of the $[Ni(dmit)_2]^-$ anion typically yielded a linear antiferromagnetic Heisenberg chain,[13] whereas the uniform 1D chain through the lateral sulfur∼sulfur contacts between the $[Ni(dmit)_2]^-$ anions yielded a ferromagnetic interaction.

Conclusions

Hydrogen bonding molecular assemblies between anilinium (Ph−NH_3^+) or adamantylammonium (AD−NH_3^+) and bulky crown ethers of dibenzo[18]crown-6 (DB[18]crown-6) or *meso*-dicyclohexano[18]crown-6 (DCH[18]crown-6) formed supramolecular rotators in $[Ni(dmit)_2]^-$ salts ($dmit^{2-}$ is 2-thioxo-1,3-dithiole-4,5-dithiolate). Different types of crystalline rotators, namely, a 180° flip-flop rotator of Ph−NH_3^+

(25) (a) Duffy, W., Jr.; Barr, K. P. *Phys. Rev.* **1968**, *165*, 647. (b) Hall, J. W.; Marsh, W. E.; Weller, R. R.; Hatfield, W. E. *Inorg. Chem.* **1981**, *20*, 1033.

and a 120° symmetrical rotator of AD−NH_3^+, were constructed on the bulky DB[18]crown-6 and DCH[18]crown-6 stator units. Because of the isotropic molecular structure of the adamantyl group, the potential energy barrier for the rotation of the adamantyl group was lower than that of the phenyl ring. The 2-fold symmetrical intermolecular interaction between the π plane of Ph−NH_3^+ and sulfur atoms of $[Ni(dmit)_2]^-$ anions yielded a 2-fold symmetrical potential energy curve with a relatively large potential energy barrier. The bulky crown ethers (DB[18]crown-6 and DCH[18]crown-6) served to keep the crystalline space for the rotators. The potential energy barriers for the rotation of the adamantyl group in (AD−NH_3^+)(DB[18]crown-6) and (AD−NH_3^+)(DCH-[18]crown-6) supramolecular cations were extremely low. They were comparable to the rotation barriers of ethane and butane and lower than that of adamantane in the plastic crystalline state. The adamantyl group was effective in constructing the rotation environment in the solid state. The structure of the supramolecular rotators directly affected the $[Ni(dmit)_2]$ arrangements and the magnetic behavior. 2D $[Ni(dmit)_2]^-$ anion arrangements were observed in (Ph−NH_3^+)-(DB[18]crown-6) and (AD−NH_3^+)(DB[18]crown-6) cations, whereas 1D lateral $[Ni(dmit)_2]^-$ interactions through the sulfur−sulfur contacts were observed in (Ph−NH_3^+)(DCH[18]crown-6) and (AD−NH_3^+)(DCH[18]crown-6) cations. A uniform 1D magnetic interaction through the lateral sulfur−sulfur contacts resulted in a ferromagnetic interaction in salt **3**. The deformation from the uniform chain of salt **2** to salt **4** changed the magnetic interaction dramatically, from ferromagnetic to antiferromagnetic coupling. Precise control of the $[Ni(dmit)_2]^-$ anion arrangement is necessary to control the magnetic properties in the solid state. On the other hand, the partially oxidized $[Ni(dmit)_2]$ anion is effective in preparing electrically conducting salts, where supramolecular rotators can be introduced as cation structures that couple with the conduction electrons.

Acknowledgment. This work was partly supported by a Grant-in-Aid for Science Research from the Ministry of Education, Culture, Sports, Science, and Technology of Japan.

Supporting Information Available: Atomic numbering scheme, structural analysis of salts **1**−**4**, calculated structural units, ^1H NMR of salt **4**, vibrational spectra, nearest neighboring packing of the rotators in salts **1**−**4**, $M - H$ curve of salt **2** at 2 K, and ESR spectra at room temperature. This material is available free of charge via the Internet at http://pubs.acs.org.

IC800271M